Characterization of Line-of-Sight Link Availability in Indoor Visible Light Communication Networks Based on the Behavior of Human Users

VOLKAN RODOPLU[ID]1, **(Member, IEEE), KEMAL HOCAOĞLU**[ID]1, **ANIL ADAR**[ID]2, **RIFAT ORHAN ÇIKMAZEL**[ID]1, **ALPER SAYLAM**[ID]1

[1]Department of Electrical and Electronics Engineering, Yaşar University, İzmir, Turkey
[2]Department of Information Engineering, University of Padua, Padua, Italy

Corresponding author: Volkan Rodoplu (e-mail: volkan.rodoplu@yasar.edu.tr)

ABSTRACT We characterize the line-of-sight (LOS) link availability in indoor visible light communication (VLC) networks based on the behavior of human users. The VLC link availability is impacted by humans in three distinct ways: (1) Users turn the lights on or off in each room. (2) Users may carry mobile devices. (3) Users constitute mobile obstacles that block or shadow the channel between the transmitter and the receiver. First, we develop a mathematical framework for VLC link availability and a probabilistic model of the VLC network with respect to human behavior in indoor environments. Second, we design a realistic multi-user, indoor VLC system simulation with static and mobile VLC devices that are expected to be found in smart home environments. We present the following four sets of results: (1) We report statistics on the blockage durations of VLC links and categorize the links with respect to these statistics. (2) We demonstrate the performance of Selection Diversity versus Maximal Ratio Combining for mobile VLC devices carried by humans in a smart home setting. (3) We show that optimal LED resource allocation policies for multiple users are impacted by the VLC link blockage events caused by humans. (4) We demonstrate that the link blockage events in different rooms become dependent due to humans who transition between rooms. Based on our results, we provide new directions for the design of network architectures for indoor VLC systems.

INDEX TERMS mobility, network simulation, shadowing, Visible Light Communication (VLC), wireless networks

I. INTRODUCTION

Visible Light Communication (VLC) refers to the transmission of data via light on the 430-770 THz visible spectrum from a Light Emitting Diode (LED), whose emitted light is modulated by data, to a photodiode that serves as the VLC receiver. The main advantage of VLC for indoor communications is the significant data rate increase that VLC can potentially provide over Wi-Fi systems [1] [2]. A key challenge to overcome is the fact that the behavior of humans in indoor settings affects the availability of VLC links.

First, whenever a user turns off the lights in a room, all of the VLC links in the room become unavailable. Thus, in contrast with Wi-Fi systems, in which the transmitter is

not intermittently turned off by humans, the VLC transmitter may present frequent interruptions in its data service that is determined completely exogenously to the goals of data transmission by the behavior of humans. Second, a human may carry a mobile VLC device. In this case, the availability of the VLC link to the device will be affected by the mobility pattern of the human who carries the device. Third, humans constitute mobile obstacles that may block the VLC link or partially shadow the VLC signal, thus degrading the Signal-to-Interference-Plus-Noise Ratio (SINR) considerably.

The goal of this paper is to advance the state of the art in modeling the impact of humans in indoor VLC networks on two fronts: First, we aim to create a mathematical framework

IEEE Access

V. Rodoplu *et al.*: Characterization of LOS Link Availability in Indoor VLC Networks Based on the Behavior of Human Users

by which the key physical-layer aspects, in regard to human behavior, can be abstracted to provide an accurate model that will be useful for VLC networking at the higher layers of the protocol stack. Second, we aim to measure observables, such as link blockage durations, in a life simulation environment, in which simulated humans carry out their daily activities, such as eating at meal times, exiting and returning to home, watching TV, working at the computer, and sleeping. Based on our mathematical framework and simulation results, we then provide new directions for the design of network architectures for indoor VLC systems.

In the first part of this work (Sections III and IV), the mathematical framework that we develop centers on two key observations: (1) The VLC channel differs from the Radio Frequency (RF) channel significantly in that light cannot penetrate opaque obstacles, whereas RF signals can travel through objects as well as room boundaries. This fact implies that, unlike the RF channel, the VLC channels across rooms that are separated by opaque walls can be decoupled completely in the absence of humans (or if the human behavior were completely predictable). (2) Under a random model of human behavior, humans in an indoor space may couple the states of distinct VLC links over long observation intervals in two ways: First, the blockage of a VLC link by a human implies the absence of the simultaneous blockage of another distant VLC link (in the same room or in another room) by the same human. Second, the presence of a human who turns on the LEDs in a room implies the simultaneous absence of the same human in another room. Thus, the LED states in different rooms become statistically dependent over long observation intervals under a random model of human behavior. Our framework introduces the novel concepts that are necessary for the statement of these results in a mathematically precise setting. This mathematical framework also facilitates the discussion of the results obtained in our simulation studies.

The second part of this work (Section V) introduces a key methodological contribution to the VLC networking literature, namely that of using a life simulation environment to measure VLC link blockage durations, to understand the impact of humans on LED allocation policies, and to quantify the dependence introduced by humans in the probabilities of blockage of distinct VLC links. To the best of the authors' knowledge, this is the first work to use a life simulation environment in measuring the impact of human behavior on the availability of VLC links. The life simulation environment accurately simulates the interactions of these humans in relationship to the interior design of the spaces that they inhabit, including their interactions with the furniture, as well as their interactions, such as talking, among themselves. Such simulation thus leads to very realistic mobility patterns that accurately capture not only the mobility patterns of individual humans but also any dependencies between the trajectories of distinct humans.

In our modeling work that targets obtaining a sufficient picture for layers above the physical layer, we deliberately relinquish precision in the description of the channel impulse response (CIR) of a VLC link due to computational constraints: Running a simulation that corresponds to a real-life duration on the order of 10 days prohibits modeling the VLC channel at the level of the exact CIR for every instance of the simulation. Understanding the CIR of the VLC channel in different settings [3] [4] [5], including the case of mobile users [6], is useful for the utilization of physical-layer schemes, such as adaptive modulation. However, from a networking perspective, since VLC attains high data rates in the presence of the Line-of-Sight (LOS) component and experiences significant performance degradation in the absence of LOS [7], it suffices, as an approximation, to measure the availability of only the LOS VLC link to each smart device. While our mathematical framework for VLC link availability is general and holds even in the presence of Non-Line-of-Sight (NLOS) components, our simulations in this work focus on only LOS link availability.

We present the following four sets of results that we have obtained in our life simulation environment: (1) We report statistics on the blockage durations of VLC links and categorize the links with respect to these statistics. (2) We demonstrate the performance of Selection Diversity versus Maximal Ratio Combining for mobile VLC devices carried by humans in a smart home setting. (3) We show that optimal LED resource allocation policies for multiple users are impacted by the VLC link blockage events caused by humans. (4) We demonstrate that the link blockage events in different rooms become dependent due to humans who transition between rooms.

The results that we present in this work have the potential to impact the networking architectures and policies in VLC systems in the near future. As the design of routing, MAC-layer and cross-layer strategies for an indoor VLC network is predicated on the availability of statistics that characterize the VLC links, this work has the potential to spur research in obtaining more detailed networking metrics for VLC systems via the use of life simulation environments. We also note, however, that while this work lays the groundwork for the quantitative analysis of the impact of human behavior on VLC link availability in a life simulation environment, ultimately field measurements on indoor VLC systems are required for obtaining the actual VLC network performance.

The rest of this paper is organized as follows: In Section II, we describe the relationship of this work to the state of the art in this area. In Section III, we state the assumptions that underlie our work. In Section IV, we develop our mathematical framework. In Section V, we present our simulation methodology and results. In Section VI, we present our conclusions.

II. RELATIONSHIP TO THE STATE OF THE ART

In this section, we describe the relationship of our work to the state of the art in four regards: (1) We contrast our approach with the mobility models that have been used in modeling the effects of human blockage and shadowing in the VLC litera-

ture. (2) We explain the differences between this work and the past work that has modeled the impact of human shadowing on the physical layer. (3) We contrast our approach with those found in the millimeter-wave communications literature that also model human blockage and shadowing. (4) We describe the relationship between our work and the remainder of the techniques in the literature used in modeling individual VLC links.

First, in understanding the effects of human blocking and shadowing on the VLC channel, to the best of the authors' knowledge, all of the past work in the literature has utilized either models with no mobility of humans over the observation interval [8] [9] or *a priori*, *random* movement models: In [10], each simulated pedestrian picks a speed that is uniformly distributed on the interval $[0, 4]$ km/h and a direction that is uniform over $[0, 2\pi]$ and walks for 5 seconds, before the same selection is repeated. In [11], two probabilistic mobility models are utilized: Under the random walk model, a human picks a direction that is uniformly distributed on $[0, 2\pi]$. Under the "main spot" model, the probability that a human sits at a particular location on the two-dimensional (2D) plane is modeled as a 2D Gaussian random variable with a higher probability density at certain main spots such as sofas and desks. In [12], humans enter a single room according to a Poisson process, where the rate of the Poisson process is varied. In addition, two scenarios are analyzed in the presence and absence of a single static obstacle in the single room. In [13], each human picks a speed randomly in $[0, 5]$ km/h and moves according to a random walk model in a single room as follows: At each instance in time, every human chooses, independently of all of the other humans, each of the 8 equiangular directions with equal probability for an office room, and 6 for a corridor. Similarly, in [14], every human moves by picking a direction uniformly on $[0, 2\pi]$ in a single room scenario. In contrast with all of this past work, we utilize the realistic mobility patterns of simulated humans that move over multiple rooms in a life simulation environment. We collect statistics on the VLC links, *not* based on a priori, assumed random movement models, but rather based on the life simulation environment.

Second, the past work has focused on modeling the impact of humans on the VLC physical layer, in particular, on the CIR of the VLC channel: In [6], the impact of user movement on the path loss and the delay spread was evaluated for three user trajectories in a living room, where the human user traverses the living room end-to-end linearly. In [15], a detailed analysis of the size and shape of an obstacle on the CIR was given. In [16], [17], [18] and [19], the impact of the reflectivity of the human as well as the receiver orientation on the CIR and the outage probability for different data rates was measured using ray tracing. Furthermore, in [20], the effects of LOS blockage, transmitter viewing angle and the receiver aperture size on the CIR of an underwater VLC link was measured in a ray tracing simulation. In contrast with these studies, in this work, we obtain statistics on the impact of humans on the LOS VLC link blockage durations, handoff

decisions, data rates under LED allocation policies, and on the probabilistic coupling of distinct VLC channels in an indoor setting.

Third, we contrast our approach with the techniques in the past work that has modeled human body blockage and shadowing in millimeter-wave cellular networks: In [21], humans are represented as cylinders with arbitrarily distributed heights and radii, whose centers follow the Poisson Point Process in two dimensions. By employing tools from stochastic geometry, the blockage probability of the LOS path is derived. In [22], the effects of human body blockage on the electric field distributions are obtained for standing and sitting human posture models in the absence of any mobility in an indoor setting. In [23], the distributions of the received signal levels as a function of frequency are reported in the presence of human body blockage. In contrast with the millimeter-wave techniques employed in these works, we measure the blockage of VLC LOS links directly based on the geometric configuration of a human relative to the LEDs in a life simulation environment.

Fourth, we note that the Shadowing Ray Tracing (SRT) algorithm in [24] is more detailed than the Lambertian radiation pattern that we employ; however, measurements there have been made in a laboratory setting in order to test the ray tracing model. In contrast, our aim is to understand the effects of realistic human behavior in indoor settings such as smart homes. A bimodal Gaussian distribution with a wide field of view (FOV) was utilized in [25] in order to model shadowing. We plan to incorporate such advanced shadowing models to our simulation environment in our future work. Furthermore, we do not currently model the effects of device misalignment, as found in [26] and [27], or the improvements obtained by the users' adjusting their own orientation [28] in order to aid the VLC network.

III. ASSUMPTIONS

In this paper, we focus on an indoor VLC system with humans (which shall also be called "users") and devices. The region on which we shall collect data is denoted by R, where a "region" is any segment of an indoor space, such as a room, apartment, office, or an apartment building or an office building. (There are no restrictions on the number of floors.) The region is considered to be a "control volume" in the sense that it is the volume on which we make all of our observations. Humans and devices may leave or enter the region; hence, the system is not assumed to be a closed system.

We classify the devices into three types: static, portable and mobile. Static devices do not move; portable devices may move but are used only when they are not in motion; mobile devices move and may be used at any time.

We assume that a VLC network has been deployed over R. The network consists of a set $\mathcal{L}$ of LEDs, each of whose location is fixed in R and a set $\mathcal{D}$ of devices that appear for at least some time in R over the observation time interval $\mathcal{T}$. The sets of static, portable and mobile devices are denoted

IEEE Access

V. Rodoplu *et al.*: Characterization of LOS Link Availability in Indoor VLC Networks Based on the Behavior of Human Users

by $\mathcal{D}_s$, $\mathcal{D}_p$, and $\mathcal{D}_m$, respectively, which are disjoint subsets that make up $\mathcal{D}$. The set of humans that appear for at least some time in R over $\mathcal{T}$ is denoted by $\mathcal{H}$. We assume that humans and the mobile devices that they carry are the only mobile objects in R; the geometric configuration (namely the location and the angular orientation) of all other objects in R is fixed.[1]

We assume that the VLC system is comprised of only the set of downlinks from the LEDs to the devices; that is, there is no uplink VLC transmission. We let $\mathcal{D}_f$ denote the subset of devices that have a feedback mechanism to the network. Such feedback might be enabled e.g. via an uplink implemented in a non-VLC technology (such as Wi-Fi [29], ZigBee [30], or their variants).

IV. MATHEMATICAL FRAMEWORK

Our goal in this section is to develop a mathematical framework based on which we analyze the states of the VLC links across the entire observation region R. The culmination of this framework will be the formal characterization of the effect of human behavior on the states of these VLC links. These theoretical foundations will then facilitate the analysis of the empirical results that will be presented in Section V.

Throughout this work, "human behavior" designates human behavior *only* as regards its effects on the states of VLC links. We note that humans affect the states of these VLC links by turning LEDs on or off, by carrying mobile devices that are VLC receivers, and by blocking VLC links[2].

We shall give an overview of the mathematical framework that appears in Sections IV-A to IV-C below, before we state it precisely. In our framework, first, we introduce the novel concept of an "LED domain." Roughly speaking, an LED domain at any given time is a set of LEDs such that every pair of LEDs in this set share at least a single spot that both of the LEDs in that pair illuminate at that time. By identifying which pairs of LEDs are related to each other in this manner, we can discover which VLC channels are potentially coupled. Conversely, by identifying which VLC channels are completely decoupled at any given time, we will show (in Section IV-C1) that the set of all VLC channels in R can be decomposed across these LED domains. This result holds either in the case where no humans are present in R for the entire $\mathcal{T}$ or if the human behavior (as defined above) is completely predictable during $\mathcal{T}$. The reason for stating this result first is to set the stage to characterize the effects of *random*[3] human behavior on the state of VLC links. Subsequently, in Section IV-C2, we describe how a random model of human behavior introduces statistical dependence

---

[1]The reason for this assumption is that we aim to isolate the effects of mobile humans on the set of VLC links.

[2]We note that humans' mobility patterns do not suffice in completely determining their behavior, since their turning LEDs on or off is, in general, related to but not completely determined by their mobility patterns.

[3]We use the term *random*, in the rigorous sense of the term, which means that a probability measure can be ascribed to the events. We do *not* imply that any particular, a priori, random model is employed to generate the mobility patterns of humans or the times at which humans turn LEDs on or off.

between VLC channels. This statistical dependence is then empirically demonstrated in Section V-B4.

Second, in Section IV-B, we define "VLC link availability." Even though in the simulations in Section V-B1, we shall demonstrate the empirical statistics on the blockage duration of VLC links without regard to the particular application that runs on any given VLC link, the framework in Section IV-B serves as a foundation for modeling LOS link blockage based purely on geometric considerations in our simulations. To this end, in the second part of Section IV-B, we mathematically distill the physical characteristics that are of consequence to the availability of VLC links.

A. LED DOMAIN

VLC is different from RF communication in that the range of a signal from an LED is delimited by the geometric configuration of objects. Throughout this paper, we assume that each LED transmits at a fixed power level when it is on; that is, we do not assume any dimmer LEDs. However, the transmit power levels may vary across different LEDs. We define the "signal range" $\mathcal{F}_l(t)$ of LED l at time $t \in \mathcal{T}$ as the set of 3D positions $(x, y, z) \in R$ at which the VLC receiver can be located such that a non-zero signal from l is received at (x, y, z) at time t. (Note that under this definition, no signal is received at any location from an LED at time t if the LED is off at time t.)

We form a time-varying, undirected graph $U(t)$, whose vertex set is $\mathcal{L}$ (as defined in Section III) and whose edge set is determined as follows: At each time t, an edge between vertices l_1 and l_2 is drawn if and only if $\mathcal{F}_{l_1}(t) \cap \mathcal{F}_{l_2}(t) \neq \emptyset$.

We define an "LED domain" at time t as a set of LEDs each of which is connected by a path on $U(t)$. (Note that at any given time t, if each of the pairs of LEDs (l_1, l_2) and (l_2, l_3) is path-connected on $U(t)$, then the pair (l_1, l_3) is also path-connected on $U(t)$.) We let $\mathcal{I}_k(t)$ denote kth LED domain of $\mathcal{L}$ at time t. Note that at each time $t \in \mathcal{T}$, the collection $\{\mathcal{I}_k(t)\}$ over k partition $\mathcal{L}$.

B. VLC LINK AVAILABILITY

In this section, we aim to characterize the link availability from each LED to each device. We assume that one or more applications, served by the VLC downlink, run on each device. Each such application a has its own Quality of Service (QoS) constraints. For simplicity, we focus only on achieving a target probability of error for each application a. (We do not model other QoS constraints.) We let γ_a denote the minimum downlink SINR, measured at the output of the demodulator, that is required to achieve a target probability of error for application a.

We say that the link $l \to i$ from LED l to device i is "available" at time t for application a, if the SINR at time t on link $l \to i$, denoted by $\text{SINR}_{l \to i}(t)$, is at least γ_a. Otherwise, we say that the link $l \to i$ is unavailable at time t for application a. (Note that the availability of link $l \to i$ at time t for application a depends on the actual data transmitted from LED l as well as the interfering signals received at i from the other LEDs in $\mathcal{L}$.)

There are two sources that clearly affect SINR. First, if LED l is off at time t, then $\mathrm{SINR}_{l \to i}(t) = 0$ for all i at time t; thus, link $l \to i$ is unavailable for all i at time t in this case. Hence, the state of each LED, which is typically determined by humans' turning lights on and off, impacts link availability. Second, let $\mathrm{SINR}_{l \to i}^{(0)}(t)$ denote the SINR of link $l \to i$ at time t in the case where LED l is on and all of the LEDs besides l are off at time t ("zero interference case"). Since $\mathrm{SINR}_{l \to i}(t) \leq \mathrm{SINR}_{l \to i}^{(0)}(t)$ in all settings, $\mathrm{SINR}_{l \to i}^{(0)}(t) < \gamma_a$ implies that $l \to i$ is not available for application a at time t. For example, if a human's body blocks the VLC link at time t, the link will be unavailable. In Section V, one of our goals will be to identify the cases for each link $l \to i$ where $\mathrm{SINR}_{l \to i}^{(0)}(t) < \gamma_a$ for all a, which will be caused typically by either the LED's being off or by a human's blocking the VLC link.

Fix the set of data transmitted by all VLC transmitters in R. (This means that the data are being sent, but it does not imply that all of the data are received correctly at the VLC receivers.) We define the "state" $S_{l \to i}^{(a)}(t)$ of link $l \to i$ for application a as a binary variable that is 1 at time t if the link is available for application a at time t and is 0 otherwise. We define the "global VLC state" as the Cartesian product of the states of all of the links in region R.

Given the fixed set of data transmitted by all VLC transmitters in R at time t, the state $S_{l \to i}^{(a)}(t)$ of a VLC link $l \to i$ for application a at time t depends only on the following factors at time t: (1) the geometric configuration and material properties of the static and mobile objects, (2) whether each of the LEDs is on or off, and (3) the shot and thermal noise at the VLC receiver of device i.

In this paper, we assume that the statistics of the shot and thermal noise are not time-varying. Fix an application a. Then, given that the data transmitted by all VLC transmitters at time t are fixed, if the position of device i at time t is $(x_i(t), y_i(t), z_i(t))$, $S_{l \to i}^{(a)}(t)$ depends only on (1) the state of each of the LEDs in the set denoted by $\mathcal{L}_i(t)$, in whose signal range $(x_i(t), y_i(t), z_i(t))$ falls, and (2) the geometric configuration and material properties of the objects that intervene the link from each such LED $l \in \mathcal{L}_i$ to device i.

C. PROBABILISTIC MODEL OF THE VLC NETWORK WITH RESPECT TO HUMAN BEHAVIOR

In this section, we develop a probabilistic model of the set of VLC links in R with respect to human behavior. First, in Section IV-C1, we show that under a deterministic model of human behavior, if the VLC channel inputs in distinct LED domains are jointly independent, then the VLC outputs across those LED domains are also jointly independent. Second, in Section IV-C2, under a random model of human behavior, we describe how the VLC channel outputs become statistically dependent. We note that this statistical dependence can be measured only over observation intervals that are long enough such that humans transition across the rooms many times. In Section V-B4, we shall present empirical support for (1) the decoupling of VLC channels on distinct

LED domains on which no human enters or leaves any LED domain under observation, and (2) the statistical dependence introduced when humans transition between rooms over a long observation interval.

1) Under a Deterministic Model of Human Behavior
First, we assume a deterministic model of human behavior.[4] Under this model, the evolution of the states of the LEDs in R as well as the shadowing caused by humans is deterministic. In this case, the only sources of randomness are (1) the signal sent on each of the LEDs, and (2) the shot and thermal noise at each VLC receiver.

Let $X_{l \to i}(t)$ and $Y_{l \to i}(t)$ denote the input to and the output of the VLC link $l \to i$, respectively, at time $t \in \mathcal{T}$. Across all VLC links in R at time t, let $\mathbf{X}(t)$ denote the vector of $X_{l \to i}(t)$, and let $\mathbf{Y}(t)$ denote the vector of $Y_{l \to i}(t)$. Let $\mathcal{K}(t)$ denote the set of LED domains in R at time t. Index the LED domains in R by $k \in \mathcal{K}(t)$. Across all VLC links in LED domain k, let $\mathbf{X}^{(k)}(t)$ denote the vector of $X_{l \to i}(t)$, and let $\mathbf{Y}^{(k)}(t)$ denote the vector of $Y_{l \to i}(t)$. If the vectors $\mathbf{X}^{(k)}(t)$ are jointly independent across the LED domains $\mathcal{K}(t)$, then, by definition of an LED domain and by the independence of the noise processes at distinct receivers,

$$\mathbb{P}\{\mathbf{Y}(t) \in d\mathbf{y}\} = \prod_{k \in \mathcal{K}(t)} \mathbb{P}\{\mathbf{Y}^{(k)}(t) \in d\mathbf{y}_k\}$$

where $\mathbf{y}_k$ is comprised of those components of $\mathbf{y}$ that fall in LED domain k.

For example, consider a smart home where all of the doors of the rooms have been shut and all of the room boundaries are opaque. Then, the set of LEDs in each room constitute an LED domain at that time. In a typical scenario, the data sent to devices in different LED domains will be independent. Then, the joint probability density function of the output vector of the links in the entire smart home decomposes into the product of the joint probability density functions of the output vectors in different rooms. However, if a door is opened into the corridor, and the LEDs in the room and the corridor are on, then the LED domains of the room and the corridor must be adjoined. Despite such possible coupling at certain times, compared with RF channels, it is significant that the set of VLC channels decompose over rooms in many practical indoor settings. In addition, VLC channels typically decompose across all of the floors of a building.

2) Under a Random Model of Human Behavior
If the behavior of the set of humans $\mathcal{H}$ in R, comprised of the trajectories of the humans and their actions, is assumed to be random, then the VLC channel outputs across different rooms become dependent. The reason is that the behavior of humans introduces dependence between the VLC channels in different rooms in two ways: (1) The presence of a human

---

[4]Such a model would be applicable in the cases where such behavior is completely predictable. Since such behavior is not completely predictable in practice, the results in this section are the limiting case of increasingly more accurate prediction.

IEEE *Access*

V. Rodoplu *et al.*: Characterization of LOS Link Availability in Indoor VLC Networks Based on the Behavior of Human Users

who turns on the LEDs in a given room implies that the same human cannot simultaneously turn on the LEDs in another room. (2) The presence of a human who blocks a VLC link in one room implies the absence of the blockage of a VLC link by the same human in another room. Either of these facts introduces dependence between the VLC channels in different rooms.

In order to isolate the effects of humans on the global VLC state, we define each of the following as a "human-caused event": (1) A human turns on or off an LED in R, and (2) a human blocks or partially shadows a VLC link in R. We define a "coherence block" as the time interval between successive human-caused events that occur within $\mathcal{T}$ in R. We let $\tilde{S}_l(t)$ denote the state of the LED at time t. In this work, $\tilde{S}_l(t) \in \{\text{ON, OFF}\}$. We let $B_{l \to i}(t)$ be a binary variable that is 1 if the link $l \to i$ is blocked or shadowed by a human and is 0 otherwise. Then, within each such coherence block, if the $\tilde{S}_l(t) \, \forall l \in \mathcal{L}$ and the $B_{l \to i}(t) \, \forall (l,i) \in \mathcal{L} \times \mathcal{D}$ are known, then the global VLC channel state is given by the model in Section IV-C1.[5] That is, in this case, the model in Section IV-C1 can be used in each coherence block, while a separate probabilistic model characterizes the transitions between the states given by the set of $\tilde{S}_l(t)$ and $B_{l \to i}(t)$ due to human-caused events.[6]

In Section V-B4, we will follow up on the implications of this mathematical model and show empirically that the blockage events of VLC links in distinct rooms in a smart home environment become statistically dependent. Since humans are the only mobile obstacles in our simulations, we will infer that this statistical dependence has been caused by humans.

V. RESULTS
In this section, first, we describe our set-up and methodology for data collection in a life simulation environment, in which simulated humans carry out their daily activities in a smart home environment. Second, we present the empirical results that we have obtained in this environment.

We first give an overview of this section: In Section V-B1, we present our results on the VLC link blockage statistics. Since the simulated humans are the only mobile obstacles in our simulations, all such blockages are caused directly by these humans. Sections V-B2 and V-B3 go beyond VLC link availability as follows: In Section V-B2, we discuss our results that show the limited advantage that Maximal Ratio Combining provides over Selection Diversity for a mobile device carried by a human in an L-shaped corridor. This specific example also serves to highlight the difference between VLC and RF communication. Even though our model uses the Lambertian radiation pattern and accounts for only the LOS components from the LEDs, the results provide an approximation to what would be obtained under the more

accurate channel models, discussed in Section II. Our results also provide an illustration of the extent to which simulations that model only the LOS component at a fixed (upwards) receiver orientation can be used in this case. In Section V-B3, we illustrate the effects of human behavior on LED allocation policies, albeit under the same aforementioned conditions. Our results demonstrate the performance of two policies (Max-Sum Data Rate Policy and the Max-Min Data Rate Policy) under the effects of human blockage of VLC links to static devices and the device mobility due to the motion of the human user. Finally, in Section V-B4, we present empirical results that support the model developed in Section IV-C.

A. METHODOLOGY
1) General Simulation Set-up
First, we designed a smart home, using the Revit® design tool (Version 2020) [31], as shown in Fig. 1. The smart home is 20 m. long, 13 m. wide, and 3.5 m. high. In this home, there are three humans: a father, a mother, who are adults, and their child, who is a young adult (aged 19 - 25). The height of each human is 1.60 m. The static (i.e. non-moving) smart devices in this home along with the rooms in which they are located are as follows: (1) kitchen (lower left-hand corner): coffee machine, refrigerator, fire alarm, curtain, (2) parents' bedroom (upper left-hand corner): curtain, fire alarm, mirror, (3) living room (lower right-hand corner): TV, two curtains, (4) study (lower middle): personal assistant, curtain, Personal Computer (PC), fire alarm, (5) bathroom (upper middle): fire alarm, speaker, mirror. In each of these five rooms, there is a single LED, except for the living room, in which there are two LEDs. In addition, there is an L-shaped corridor in the middle of the home with two LEDs. Furthermore, the young adult's bedroom, which appears in the upper right-hand corner of the figure, has a single LED.

In Fig. 1, one human is in the kitchen, one in the corridor[7], and one is watching TV in the living room. Each of the three humans carries a mobile phone, which is assumed to be attached to that human at all times. (We plan to model humans' leaving and picking up their phones in our future work.) All of the (static and mobile) devices are assumed to face up to the ceiling at all times. (We shall model time-varying device angles for mobile devices in our future work.)

In Fig. 1, whenever an LED is on, if the link from that LED to a mobile device is not blocked, a white Line-of-Sight (LOS) link is drawn between the LED and the mobile device; furthermore, if the link from that LED to a static device is not blocked, a green LOS link is drawn between the LED and the static device. If an LED is on and the link from that LED to a device is blocked, a red LOS link is drawn. Each red LOS link indicates that the link is not available at this time. (An example of such a red LOS link is the one from LED8 to the coffee machine in the snapshot of the smart home taken in Fig. 1. The red LOS link indicates that the link is currently

---

[5]The model in IV-C1 is more general in that it includes not only the case where the links are not impacted by human behavior but also the case where such impact is completely predictable.

[6]This probabilistic model need *not* be a Markov chain. The empirical investigation of the exact probabilistic model that characterizes the transitions between these states is beyond the scope of the current paper.

[7]A silhouette of this human in the corridor has been shown, as the human turns the corner, at each of the two instances that are separated by approximately 2 seconds.

V. Rodoplu *et al.*: Characterization of LOS Link Availability in Indoor VLC Networks Based on the Behavior of Human Users
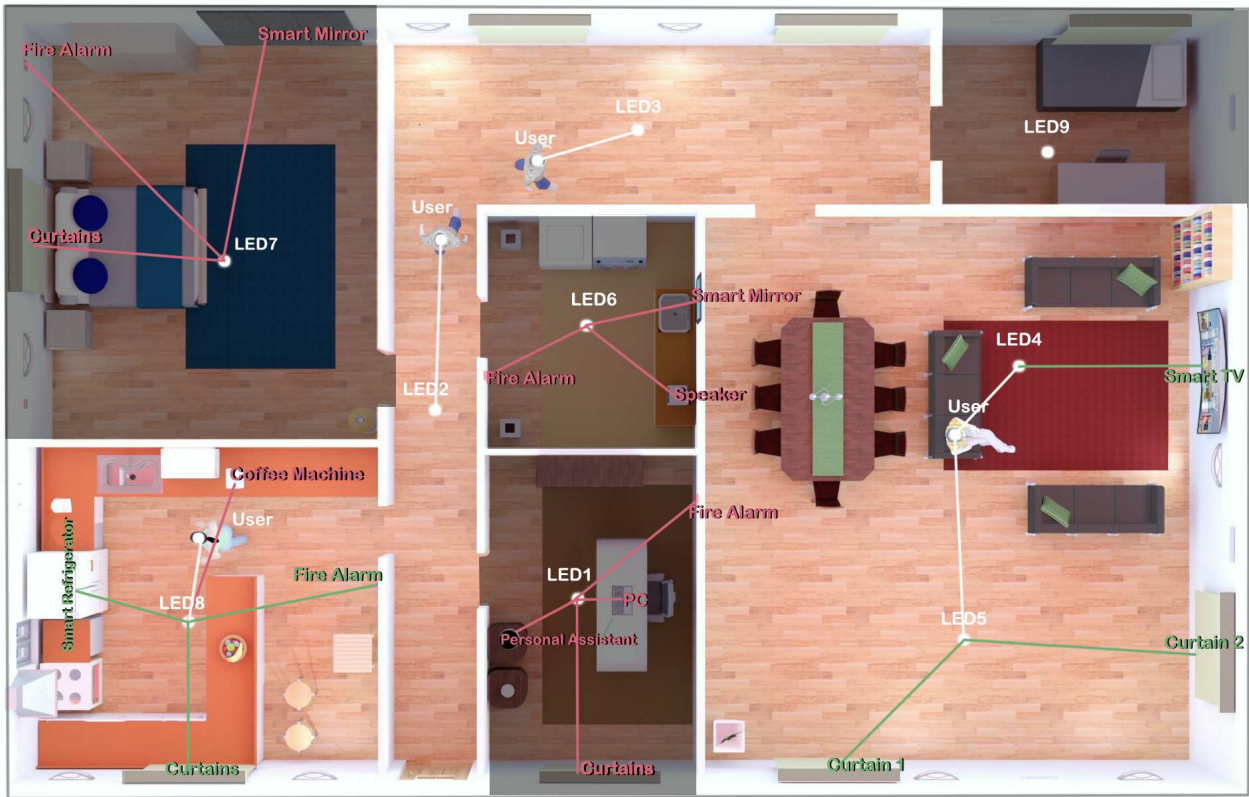
IEEE *Access*

FIGURE 1: The smart home set-up with static and mobile devices, to each of which there is a VLC downlink

blocked, in this case by a human who intervenes the link.) Furthermore, in those rooms in which the LED is off, a red LOS link is drawn between the LED in that room and the devices in that room in order to indicate that those VLC links are unavailable. (In this case, each red LOS link shows a VLC link that would form if the LED were turned on.) We note that we have set the locations of the static devices in this home such that if the LEDs are on in a given room, unless a human intervenes, a LOS link exists to each static device from some LED that is on in that room.[8]

Second, we set up the smart home that we have designed in the FreeSO simulator (Version beta/update-79a) [32]. The three simulated humans were created as a family that is comprised of a father and a mother, and their child (modeled as a young adult). All of the other aspects of these humans, such as their outer appearance, which are not related to the human behavior modeled in this work, were chosen at random. Our simulation models the behavior of these humans for a total of 13 simulated days from 8 AM of the first day to 12 AM at the end of the 13th day. In the simulation, the humans carry out their daily activities, such as eating at meal times, exiting and returning to home, watching TV, working
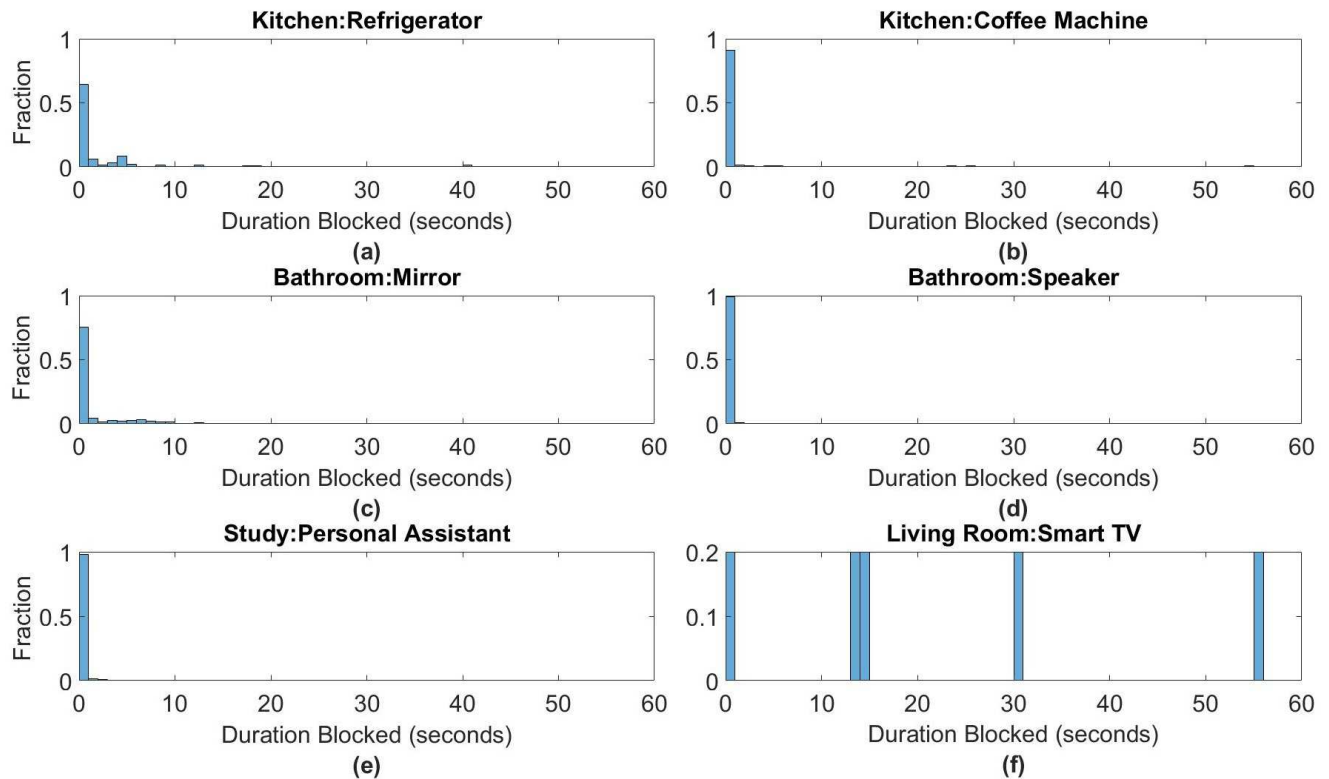
at the computer, and sleeping.

Whenever at least one human is present in a room, all of the LEDs in that room are on, and all of the LEDs in that room are off otherwise. (Thus, this simulation assumes that the daylight outside is not sufficient; hence, the LEDs are typically turned on even during the day as well. We shall model human behavior in relation to the amount of daylight present in each room in our future work.)

2) VLC Link LOS Channel Model

Based on the reasons stated in Section I, in this work, we model only the LOS component of each VLC link. That is, $Y(t) = \beta X(t - \tau_{LOS}) + N(t)$, where $Y(t)$ is the output of the link, $X(t)$ is the signal transmitted by the LED, β is the channel gain, τ_{LOS} is the delay of the LOS component, and $N(t)$ is the sum of the shot and the thermal noise at the VLC receiver. Since the deterministic part of the channel is given by $h(t) = \beta\delta(t - \tau_{LOS})$, the channel DC gain $H(0)$, which is the Fourier transform of $h(t)$ at the DC frequency, equals β.

The channel DC gain is calculated via the Lambertian radiation pattern, given in [33] [34]. The parameter values for our simulation were set as follows: The physical area of the photo detector is 9 mm^2, and the half-power semi-angle is 60°. Since all our receivers face up to the ceiling, for any given VLC link, the angle of irradiance ϕ and the angle of incidence ψ of that link (with respect to the vertical line

---

[8]If there is no VLC downlink to a static device from any LED when the LEDs in a given room are on, the device can be eliminated from our study, since we examine the effects of blockage events caused by humans on VLC links.

IEEE *Access*

V. Rodoplu *et al.*: Characterization of LOS Link Availability in Indoor VLC Networks Based on the Behavior of Human Users

FIGURE 2: Normalized histograms of the blockage durations (in seconds) of VLC links to smart devices: (a) refrigerator (kitchen) [235 samples], (b) coffee machine (kitchen) [329 samples], (c) mirror (bathroom) [619 samples], (d) speaker (bathroom) [110 samples], (e) personal assistant (study) [145 samples], (f) television (living room) [5 samples] (Each histogram has been normalized with respect to the total number of samples for that particular smart device.)

drawn at the LED and the device, respectively) are equal. Furthermore, both the optical concentration gain $g(\psi)$ and the optical filter gain $T_s(\psi)$ are equal to 1 $\forall\psi$. All of the LEDs in our simulations are assumed to transmit at 1 Watt. The total noise power at each VLC receiver is taken to be 4.35×10^{-6} Watts, which was computed based on [33]. We assume On-Off-Keying (OOK) modulation with a signaling rate of 10 MHz.[9]

B. SIMULATION RESULTS

In this section, our goal is to present simulation results that have direct bearing on VLC network design.

1) Blockage Durations of Individual VLC Links to Static Devices

We use the general simulation set-up (described in Section V-A1) and obtain results over the entire duration of the simulation. In Fig. 2, we show the normalized histogram for the duration for which a VLC link to a static device is blocked by humans, measured only over those times at which each LED in the given room is on, for all VLC links that exhibit at least one blockage event. The LED from which each of these VLC links emanates is shown in Fig. 1. The total number of

---

[9]The exact values of the noise power and the signaling rate do not affect our simulation results in Sections V-B1 and V-B4. While the quantitative results in Section V-B2 are impacted when the noise power changes, and those in Section V-B3 are impacted when the signaling rate and the noise power change, the demonstrated qualitative nature of the impact of human blockage in these latter sections and the main conclusions drawn therein remain invariant.

samples for each normalized histogram in Fig. 2 is given in the caption of Fig. 2. We also note that the bin width for each normalized histogram is 1 second.

With regard to the empirical distribution of blockage durations, we classify all VLC links in our simulation into four mutually exclusive categories that span all possibilities. These categories are detailed below.

Our first category consists of those links for each of which no blockage events were observed in our simulation because each of these devices had been installed at a sufficiently high location such that the VLC link from the LED to the device was not interrupted. (The normalized histograms for this category are not shown in Fig. 2, since these histograms are empty.) The links to all of the fire alarms and the curtains comprise this category in our simulation.

Our second category consists of those links for each of which a significant fraction (taken to be greater than 0.9) of the observed blockage durations are less than 1 second. The links to the coffee machine in the kitchen (Fig. 2(b)), to the speaker in the bathroom (Fig. 2(d)), and to the personal assistant in the study (Fig. 2(e)) fall in this category. A significant fraction of the blockage durations for these links is less than 1 second because the simulated humans typically pass quickly when they are in front of these devices. (We note, however, that in our results, there are blockage events observed for the coffee machine that last approximately 24, 26, and 55 seconds. These events occur when a human lingers in front of the coffee machine.)

IEEE Access

V. Rodoplu *et al.*: Characterization of LOS Link Availability in Indoor VLC Networks Based on the Behavior of Human Users

Our third category consists of those links for each of which there are non-negligible tails (whose total fraction is at least 0.1) that extend beyond 1 second, but such that at least half of the entire set of observed blockage durations for that link are less than 1 second. The links to the refrigerator (Fig. 2(a)) and to the mirror (Fig. 2(c)) fall in this category. In the figure, we observe that these tails extend to approximately 41 seconds for the refrigerator and to 13 seconds for the mirror. The tails are caused by the blockage events that occur when the simulated humans linger in front of the refrigerator in the kitchen (e.g. as they get food from the refrigerator) and in front of the mirror in the bathroom (e.g. when they brush their teeth).

Our fourth category consists of those links for each of which less than half of the total number of observed blockage durations are less than 1 second. In our simulation, only the link to the smart TV (Fig. 2(f)) falls in this category. A blockage event for the link to the smart TV occurs when a human stands in front of the smart TV, thus blocking its LOS link.[10]

The implication of these results for VLC network design is that for static devices that have a mechanism for feedback to the network, the VLC network can optimize the re-transmission attempt intervals at the Data Link Control (DLC) Layer as follows: Once the VLC link to a device goes into outage (i.e. the link is blocked), based on the distribution of the blockage duration and the delay constraint of the application, the network can decide on the timing of the next re-transmission attempt to that device.[11]

2) Selection Diversity versus Maximal Ratio Combining for Mobile Devices Carried by Humans

We shall examine a particular segment in the simulation in which a mobile device, which is carried by a human who traverses the corridor, retains downlink VLC connectivity via two different mechanisms: Selection Diversity, in which the mobile device remains connected to the LED that has the highest downlink Signal-to-Noise Ratio (SNR) and thus performs hard handoff, and Maximal Ratio Combining (MRC) in which the mobile device optimally combines the signals from all LEDs in the LED domain in which the mobile device appears. While these mechanisms are well-known for RF communication, our aim is to examine the resulting SNR as a function of time in our simulation setting. For MRC, we assume that the VLC network has the ability to synchronize transmissions from the LEDs on the downlink at the resolution of a baseband symbol (assuming that OOK modulation is used).

We display the results for a real-life duration of 10 seconds. In this simulation segment, the young adult walks northwards through the L-shaped corridor in Fig.1, starting at its lower end, takes the right turn in the middle, and continues
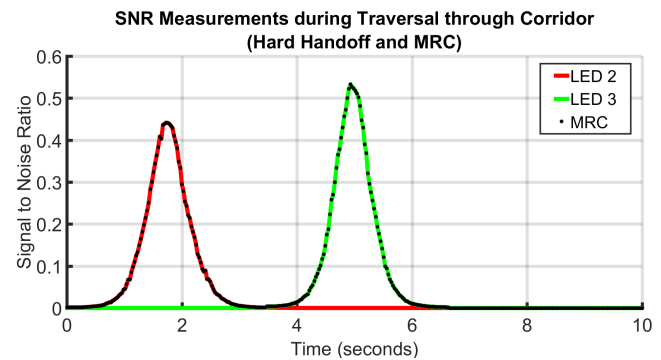
FIGURE 3: The variation of SNR as a function of time for the link from LED2 to the mobile device (shown in red) and for the link from LED3 to the same mobile device (shown in green), compared with that under MRC (shown in black) from both LEDs to the mobile device

eastward in the corridor until he exits into his bedroom, maintaining roughly constant speed through the corridor. Fig. 3 shows the SNR on his phone (obtained according to the Lambertian radiation pattern) from each of the two LEDs in the corridor, as well as what would be obtained under MRC from these two LEDs. (In Fig. 3, we graph the magnitude of the SNR *without* converting it into decibel (dB).) We see that first, as opposed to RF communication which would penetrate through walls, the signal from each LED is sharply delineated by the opaque walls of the corridor. A significant consequence is that there is only a limited area in the corridor on which the signal from both LEDs can be received successfully and combined as in MRC. Hence, we see that MRC may be applicable over much more restricted spaces for VLC than for RF communication. Second, we see that the SNR for the signal from each LED has a concave shape produced when the mobile device moves at roughly constant speed. The peak is the point where the mobile device passes under the LED, and the curvature of the shape can be used in analytical fits to estimate at which points the SNR will be above the acceptable threshold for a given application in a VLC network[12]. Third, we see that hard handoff (under Selection Diversity) and MRC have comparable SNR performance due to the fact that the two LEDs in the corridor are not co-visible by the mobile device except when the mobile user is at the corner of the corridor. When we zoom into Fig. 3 around the point at which hard handoff is performed, as shown in Fig. 4, we see that MRC outperforms hard handoff by 24% at the point where the maximum gain due to MRC occurs. Our overall conclusion is that VLC network architectures can decide whether to use MRC based on the SNR data collected from devices in the network and allocate network resources accordingly.

3) Effect of Humans on the Performance of LED Allocation Policies

In this subsection, our goal is to examine the effect of humans on the performance of policies based on which multiple

---

[10]We included a VLC link to a smart TV in our simulation in order to understand to what extent a downlink transmission to the TV can be supported based on VLC.

[11]A full VLC network design will be undertaken in our future work.

[12]Since our results were obtained under a fixed, upwards orientation of the VLC receiver, further studies would be necessary in order to understand the effects of random receiver orientation in this case. Such a study is beyond the scope of the current paper.
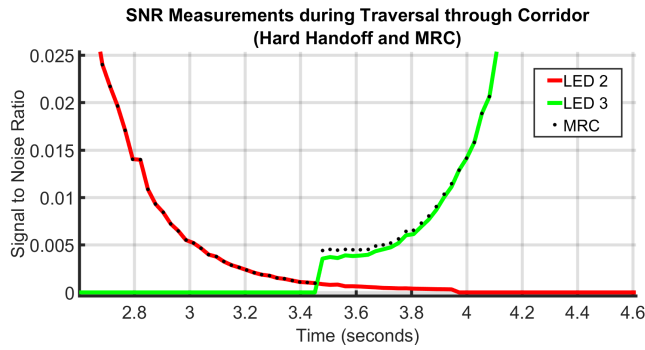
FIGURE 4: Zoom-in to Fig. 3 around the point in time at which hard handoff occurs.

FIGURE 5: The sum data rate under the Max-Sum Data Rate Policy as a function of time over the 18-second simulation segment

LEDs in an LED domain are allocated to different devices in the room. The two policies whose performance we shall test are: (1) Maximize the total data rate (which we call "Max-Sum Data Rate Policy"), and (2) Maximize the minimum data rate (which we call "Max-Min Data Rate Policy"), over all links in a given LED domain. While the Max-Sum Data Rate Policy takes a utilitarian perspective, the Max-Min Data Rate Policy is aimed at achieving fairness across the devices.[13]

We set up a separate simulation[14] in which there is a single human (with a mobile device) in the living room in Fig. 1, in addition to the three static devices (the smart TV and two smart curtains) in that room. We assume that slot synchronization has been achieved between the two LEDs in the room by the VLC network. In our simulations, we have chosen this slot duration to be $1/30$ seconds. First, we assume that each of the two LEDs in the living room (namely LED4 and LED5 in Fig. 1) transmits to at most one device in a given time slot under any policy; that is, no broadcast or multicast transmission takes place. (This is reasonable since distinct devices typically require distinct data on the VLC downlink.) Second, for each link on which data transmission takes place in a given time slot, we calculate the maximum achievable data rate based on Shannon's capacity formula for the Additive White Gaussian Noise (AWGN) channel.[15] Third, we allow the use of macroscopic diversity, in which the two LEDs, which are assumed to have been symbol-synchronized at the baseband by the network, can send the same information to a given device. We assume that MRC is used to combine these symbol-synchronized signals in this case.

We define a "link configuration" for any given time slot as a table that shows to which device (if any) each LED transmits in that slot. For the results in this section, we

assume that there is an infinite stream of data to be transmitted by the network to each device. (This assumption allows us to compare the capacity under the two policies above.) Then, under each policy, since each LED transmits to a single device and there are 4 devices, there are a total of 16 possible link configurations. In each time slot, each policy optimizes its own metric by choosing one of these link configurations. We use the following short-hand notation to index the devices in the living room: $c1$ and $c2$ denote Curtain 1 and 2, respectively; tv denotes the smart TV; m denotes the mobile device. Furthermore, when used as an index below, we shall denote LED4 by 4 and LED5 by 5. Finally, $\tilde{R}_{l \to i}$ denotes the data rate on link $l \to i$ from LED l to device i.

In Fig. 5, we display the max-sum data rate as a function of time over an 18-second window. The optimal link configuration that achieves the max-sum data rate in each time slot has also been shown in the legend of this figure. On the interval $[0, 5.1]$ seconds, the optimal link configuration is the one in which LED4 transmits to the smart TV, and LED5 transmits to Curtain 1. Throughout this interval, $(\tilde{R}_{4 \to tv}, \tilde{R}_{5 \to c1}) = (8.5, 47.3)$ Mbps. (The data rate of each device is not shown in the figure.) At $t = 0$ seconds, the father is standing in front of the sofa that appears in the lower part of the living room in Fig. 1. From $t = 0$ to 5.1 seconds, he walks towards the front of the smart TV. At $t = 5.1$ seconds, he blocks the link from LED4 to the smart TV. Since that link becomes blocked, the Max-Sum Data Rate Policy starts using LED4 in order to transmit to the mobile device carried by the father and stops transmitting to the smart TV. In contrast, LED5 continues to transmit to Curtain 1. In Fig. 5, we see that the max-sum data rate jumps to 61.4 Mbps, which is the sum of $\tilde{R}_{4 \to m}$ and $\tilde{R}_{5 \to c1}$, where $(\tilde{R}_{4 \to m}, \tilde{R}_{5 \to c1}) = (14.1, 47.3)$ Mbps. This optimal link configuration is retained on the interval $[5.1, 9.1]$ seconds. From $t = 9.1$ to 11.0 seconds, the father moves towards LED4 while continuing to block the link from LED4 to the smart TV. In Fig. 5, we see that the max-sum data rate continually increases during this interval to 67.4 Mbps. At $t = 11.0$ seconds, the father moves towards the lower sofa, hence unblocking the link from LED4 to the smart TV. Thus, from $t = 11.0$ to 15.1 seconds, LED4 transmits to the smart TV and LED5 continues to transmit to Curtain 1. On this interval, $(\tilde{R}_{4 \to tv}, \tilde{R}_{5 \to c1}) = (8.5, 47.3)$ Mbps; that is, the

---

[13]Policies in actual VLC systems are expected to be far more sophisticated than the ones presented here. Our goal is to demonstrate the results of simple policies to understand the impact of blockage by humans on the data rate.

[14]For the purposes of this section, we set up a separate simulation for only the living room in order to find a case in which the simulation segment contains both blockage of the smart TV by a human and a switch in the assignment of LEDs to particular devices.

[15]This calculation is valid in the regime where the thermal noise dominates over the shot noise for the VLC link, and serves as an approximation otherwise.
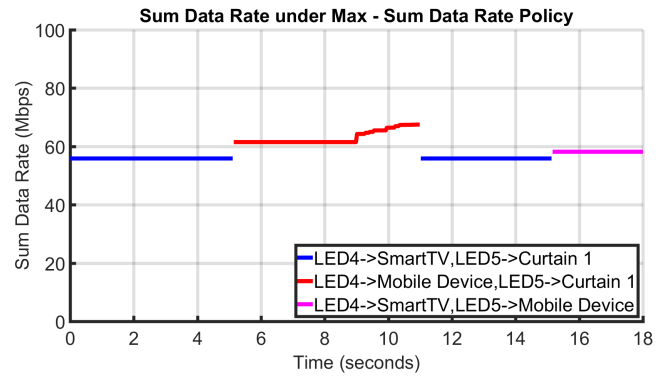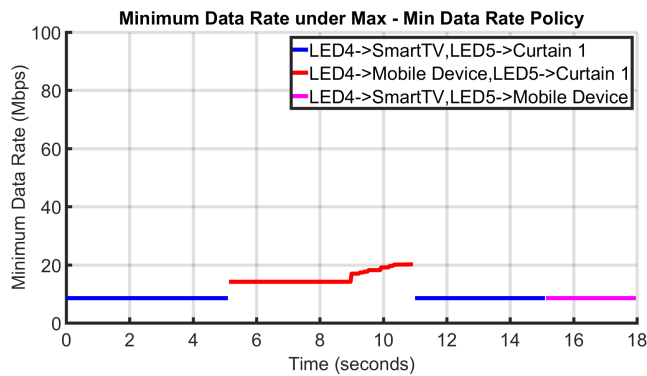
FIGURE 6: The minimum data rate under the Max-Min Data Rate Policy as a function of time over the same 18-second simulation segment as for Fig. 5

optimal link configuration returns to the initial one. During the interval $[11.0, 15.1]$ seconds, the father moves past the lower sofa towards the lower wall of the living room. At $t = 15.1$ seconds, the optimal link configuration switches the link between LED5 and Curtain 1 to the link between LED5 and the mobile device. The reason is that a higher data rate can be achieved by the LED5's transmitting on the latter link than on the former. At $t = 18$ seconds, the simulation segment terminates.

In Fig. 6, we display the max-min data rate as a function of time over the same 18-second simulation segment. We see that on the interval $[0, 5.1]$ seconds, the Max-Min Data Rate Policy uses the same link configuration as the Max-Sum Data Rate Policy. The max-min data rate that is achievable on this interval is 8.5 Mbps, which is the data rate of the link from LED4 to the smart TV. We note that the same color coding has been used to plot the results for each link configuration in Fig. 5 and Fig. 6. In Fig. 6, we see that the same sequence of link configurations is used over the 18-second segment as in Fig. 5. While Fig. 6 shows the value of the objective function, namely the max-min data rate on this simulation segment, the sum data rate achieved under the Max-Min Data Rate Policy turns out to be identical to the one achieved under the Max-Sum Data Rate policy during this simulation segment. Finally, we note that the max-min data rate during $[11.0, 15.1]$ and $[15.1, 18]$ seconds is 8.5 Mbps on both of these intervals, even though the optimal link configurations for these intervals are different (as shown in the legend of Fig. 6).

4) Empirical Results on the Probabilistic Model of VLC Link Blockage Based on Human Behavior

In this section, we report our empirical results on the probabilistic model of the blockage of VLC links with respect to human behavior, described in Section IV-C. To this end, we made measurements in two different scenarios[16]: The results on the first scenario below support the hypothesis that the blockage events of VLC links in distinct LED domains are independent when these LED domains are observed

[16]Each scenario corresponds to a particular selection of the observation interval over which measurements are collected from the original simulation described in Section V-A1.

simultaneously over time intervals in which no human exits or enters either domain. In contrast, in the second scenario, when the same VLC links in the above two LED domains are observed over the *entire* $\mathcal{T}$, the results support the hypothesis that dependence between the blockage events of VLC links in these two LED domains is introduced by the humans who transition between rooms.

Note that in our simulation (Section V-A1), whenever a human enters a room in which there is no other human, he or she turns on the LEDs in that room. Furthermore, whenever a human exits the room, if there is no other human left in the room, he or she turns off the LEDs in that room. In our scenarios, we have picked the kitchen (in Fig. 1) as the first LED domain and the bathroom as the second LED domain.

For our first scenario, we identified three simulation segments, in each of which there was a single human in the kitchen and a single human in the bathroom (simultaneously) throughout the segment. Furthermore, no human entered or exited either of these LED domains over these simulation segments. Now, if the blockage events of the VLC links in the two LED domains are independent, then the probability that the coffee machine (in the kitchen) is blocked given that the smart mirror (in the bathroom) is blocked must equal the probability that the coffee machine is blocked. In order to estimate each of these two probabilities, we measured the frequency (in discrete-time units at (1/30)-second intervals) of occurrence of each event during the simulation segment. In each simulation segment, we found that the two fractions were equal: In the first simulation segment, 7 out of 1380 samples, in the second, 6 out of 780 samples, and in the third, 9 out of 270 samples were the fractions obtained as the estimates of both the conditional and unconditional probabilities in each case. These results support the hypothesis that blockage events in distinct LED domains are independent over intervals where no human enters or exits either of these domains.

In our second scenario, we formed estimates of the same probabilities as in the first scenario, albeit over the entire simulation interval $\mathcal{T}$, by measuring the frequencies of occurrence. We found that the running frequencies converged[17] in both cases and formed estimates of the following probabilities: The probability that the coffee machine (in the kitchen) is blocked given that the smart mirror (in the bathroom) is blocked was estimated as 0.604, and the probability that the coffee machine (in the kitchen) is blocked was estimated as 0.714. The fact that these two estimated probabilities are not equal suggests that these two events are not independent. Since humans are the only mobile obstacles that change rooms in this simulation, we infer that this dependence between VLC link blockage events is caused by humans.

VI. CONCLUSIONS

We have developed a framework to characterize the VLC link availability in an indoor environment and a model by which

[17]The total number of samples collected over the entire simulation duration for this purpose was 673,000.

the impact of human behavior on VLC link availability can be quantified. Based on this framework, we presented our results on the statistics of the blockage duration of VLC links, demonstrated the performance difference between Selection Diversity and Maximal Ratio Combining in indoor settings, quantified the impact of humans' blocking VLC links on the data rate obtained under distinct LED resource allocation policies, and measured the dependence introduced by humans between VLC links in distinct LED domains.

In our future work, we plan to develop novel VLC network architectures for smart homes and offices, based on the results of this paper as follows: (1) We will develop a three-layer VLC network architecture that consists of a VLC router that routes to each LED domain, a VLC access manager that manages the access (including the use of macroscopic diversity) within an LED domain, and a VLC link manager that manages each link in a given LED domain. (2) We will develop novel LED resource allocation policies that utilize the blockage statistics of individual VLC links in an LED domain. (3) We will design a VLC Data Link Control Layer that optimizes resources by adjusting the time between retransmission attempts on each VLC link based on the blockage duration statistics for each device that has an uplink feedback mechanism to the network. (4) We will develop sophisticated access and resource allocation schemes that utilize the statistical dependence introduced by humans between the blockage events in distinct LED domains.

REFERENCES

[1] P. H. Pathak, X. Feng, P. Hu, and P. Mohapatra, "Visible light communication, networking, and sensing: A survey, potential and challenges," IEEE communications surveys & tutorials, vol. 17, no. 4, pp. 2047–2077, 2015.

[2] L. E. M. Matheus, A. B. Vieira, L. F. Vieira, M. A. Vieira, and O. Gnawali, "Visible light communication: Concepts, applications and challenges," IEEE Communications Surveys & Tutorials, vol. 21, no. 4, pp. 3204–3237, 2019.

[3] E. Sarbazi, M. Uysal, M. Abdallah, and K. Qaraqe, "Indoor channel modelling and characterization for visible light communications," in 2014 16th International Conference on Transparent Optical Networks (ICTON). IEEE, 2014, pp. 1–4.

[4] F. Miramirkhani and M. Uysal, "Channel modeling and characterization for visible light communications," IEEE Photonics Journal, vol. 7, no. 6, pp. 1–16, 2015.

[5] Y. Qiu, H.-H. Chen, and W.-X. Meng, "Channel modeling for visible light communications—a survey," Wireless Communications and Mobile Computing, vol. 16, no. 14, pp. 2016–2034, 2016.

[6] F. Miramirkhani, O. Narmanlioglu, M. Uysal, and E. Panayirci, "A mobile channel model for VLC and application to adaptive system design," IEEE Communications Letters, vol. 21, no. 5, pp. 1035–1038, 2017.

[7] M. Kashef, M. Ismail, M. Abdallah, K. A. Qaraqe, and E. Serpedin, "Energy efficient resource allocation for mixed RF/VLC heterogeneous wireless networks," IEEE Journal on Selected Areas in Communications, vol. 34, no. 4, pp. 883–893, 2016.

[8] Y. Wang, X. Wu, and H. Haas, "Analysis of area data rate with shadowing effects in Li-Fi and RF hybrid network," in 2016 IEEE International Conference on Communications (ICC). IEEE, 2016, pp. 1–5.

[9] ——, "Load balancing game with shadowing effect for indoor hybrid LiFi/RF networks," IEEE Transactions on Wireless Communications, vol. 16, no. 4, pp. 2366–2378, 2017.

[10] T. Komine, S. Haruyama, and M. Nakagawa, "A study of shadowing on indoor visible-light wireless communication utilizing plural white LED lightings," Wireless Personal Communications, vol. 34, no. 1-2, pp. 211–225, 2005.

[11] K. Xu, H.-Y. Yu, Y.-J. Zhu, and Y. Sun, "On the ergodic channel capacity for indoor visible light communication systems," IEEE Access, vol. 5, pp. 833–841, 2017.

[12] Z. Dong, T. Shang, Y. Gao, and Q. Li, "Study on VLC channel modeling under random shadowing," IEEE Photonics Journal, vol. 9, no. 6, pp. 1–16, 2017.

[13] P. Chvojka, S. Zvanovec, P. A. Haigh, and Z. Ghassemlooy, "Channel characteristics of visible light communications within dynamic indoor environment," Journal of Lightwave Technology, vol. 33, no. 9, pp. 1719–1725, 2015.

[14] X. Bao, A. A. Okine, W. Adjardjah, W. Zhang, and J. Dai, "Channel adaptive dwell timing for handover decision in VLC-Wi-Fi heterogeneous networks," EURASIP Journal on Wireless Communications and Networking, vol. 2018, no. 1, p. 244, 2018.

[15] X. Nan, P. Wang, L. Guo, L. Huang, and Z. Liu, "A novel VLC channel model based on beam steering considering the impact of obstacle," IEEE Communications Letters, 2019.

[16] C. Le Bas, S. Sahuguede, A. Julien-Vergonjanne, A. Behlouli, P. Combeau, and L. Aveneau, "Human body impact on mobile visible light communication link," in 2016 10th International Symposium on Communication Systems, Networks and Digital Signal Processing (CSNDSP). IEEE, 2016, pp. 1–6.

[17] ——, "Impact of receiver orientation and position on visible light communication link performance," in 2015 4th International Workshop on Optical Wireless Communications (IWOW). IEEE, 2015, pp. 1–5.

[18] A. Behlouli, P. Combeau, S. Sahuguède, A. Julien-Vergonjanne, C. Le Bas, and L. Aveneau, "Impact of physical and geometrical parameters on visible light communication links," in 2017 Advances in Wireless and Optical Communications (RTUWO). IEEE, 2017, pp. 73–76.

[19] C. Lebas, S. Sahuguede, A. Julien-Vergonjanne, P. Combeau, and L. Aveneau, "Infrared and visible links for medical body sensor networks," in 2018 Global LIFI Congress (GLC). IEEE, 2018, pp. 1–6.

[20] F. Miramirkhani and M. Uysal, "Visible light communication channel modeling for underwater environments with blocking and shadowing," IEEE Access, vol. 6, pp. 1082–1090, 2017.

[21] M. Gapeyenko, A. Samuylov, M. Gerasimenko, D. Moltchanov, S. Singh, E. Aryafar, S.-p. Yeh, N. Himayat, S. Andreev, and Y. Koucheryavy, "Analysis of human-body blockage in urban millimeter-wave cellular communications," in 2016 IEEE International Conference on Communications (ICC). IEEE, 2016, pp. 1–7.

[22] M. Yamagishi, T. Hikage, M. Sasaki, M. Nakamura, and Y. Takatori, "FDTD-based numerical estimation of human body blockage characteristics in 26GHz band indoor propagation," in 2018 48th European Microwave Conference (EuMC). IEEE, 2018, pp. 878–881.

[23] K. Kitao, N. Tran, T. Imai, and Y. Okumura, "Frequency characteristics of changes in received levels by human body blockage in indoor environment," in 2016 URSI Asia-Pacific Radio Science Conference (URSI AP-RASC). IEEE, 2016, pp. 373–376.

[24] Y. Xiang, M. Zhang, M. Kavehrad, M. S. Chowdhury, M. Liu, J. Wu, and X. Tang, "Human shadowing effect on indoor visible light communications channel characteristics," Optical Engineering, vol. 53, no. 8, p. 086113, 2014.

[25] H. Farahneh, C. Mekhiel, A. Khalifeh, W. Farjow, and X. Fernando, "Shadowing effects on visible light communication channels," in 2016 IEEE Canadian Conference on Electrical and Computer Engineering (CCECE). IEEE, 2016, pp. 1–5.

[26] J. Zhang, X. Zhang, and G. Wu, "Dancing with light: Predictive in-frame rate selection for visible light networks," in 2015 IEEE Conference on Computer Communications (INFOCOM). IEEE, 2015, pp. 2434–2442.

[27] Y. S. Eroğlu, Y. Yapıcı, and I. Güvenç, "Effect of random vertical orientation for mobile users in visible light communication," in 2017 51st Asilomar Conference on Signals, Systems, and Computers. IEEE, 2017, pp. 238–242.

[28] J. Beysens, Q. Wang, and S. Pollin, "Improving blockage robustness in VLC networks," in 2019 11th International Conference on Communication Systems & Networks (COMSNETS). IEEE, 2019, pp. 164–171.

[29] S. Shao, A. Khreishah, M. B. Rahaim, H. Elgala, M. Ayyash, T. D. Little, and J. Wu, "An indoor hybrid Wi-Fi-VLC Internet access system," in 2014 IEEE 11th International Conference on Mobile Ad Hoc and Sensor Systems. IEEE, 2014, pp. 569–574.

[30] C.-M. Kim, S.-I. Choi, and S.-J. Koh, "IDMP-VLC: IoT device management protocol in visible light communication networks," in 2017 19th International Conference on Advanced Communication Technology (ICACT). IEEE, 2017, pp. 578–583.

[31] Autodesk, Inc. (2019) Revit 2020. [Online]. Available: https://www.autodesk.com/products/revit/overview

[32] R. Simpson. (2019) Free Simulator Online. [Online]. Available: http://www.freeso.org/

[33] T. Komine and M. Nakagawa, "Fundamental analysis for visible-light communication system using LED lights," IEEE Transactions on Consumer Electronics, vol. 50, no. 1, pp. 100–107, Feb 2004.

[34] J. M. Kahn and J. R. Barry, "Wireless infrared communications," Proceedings of the IEEE, vol. 85, no. 2, pp. 265–298, Feb 1997.

ANIL ADAR obtained his B.Sc. degree as an honor student from the Department of Electrical and Electronics Engineering at Yaşar University in Izmir, Turkey. During his senior year, he worked as a research scholar in the Scientific Research Project "Development of Channel Models and Techniques for Visible Light Communication" at Yaşar University. His graduation project, entitled "Video Transmission via Visible Light Communication," was supported by TÜBİTAK (Scientific and Technological Research Council of Turkey) under the 2209-B Industry Focused Undergraduate Thesis Support Program. His team's low-cost VLC system design was published at the 2019 Conference on Innovations in Intelligent Systems and Applications. He is currently pursuing his Master's degree in Information and Communication Technologies for Internet and Multimedia in the Department of Information Engineering at the University of Padua in Padua, Italy. His research interests are Visible Light Communication and its applications to multimedia technologies.

VOLKAN RODOPLU is Associate Professor of Electrical Engineering and Marie Skłodowska-Curie Fellow of the European Commission at Yaşar University in Izmir, Turkey. He obtained his B.S. degree (summa cum laude) in Electrical Engineering from Princeton University in 1996, and his M.S. and Ph.D. degrees in Electrical Engineering from Stanford University in 1998 and 2003, respectively. He has worked for the Wireless Research Division of Texas Instruments (Dallas, TX) and for Tensilica Inc. (Santa Clara, CA). He served as an Assistant Professor of Electrical Engineering at the University of California Santa Barbara from 2003 to 2009, where he was promoted to Associate Professor with tenure. His current research focuses on the Internet of Things, Predictive Networks, Smart Cities, and Visible Light Communication. He is the winner of the National Science Foundation CAREER Award (USA), the University of California Regents' Junior Faculty Fellowship, Stanford Department of Electrical Engineering Outstanding Service Award, Stanford Graduate Fellowship (as Andreas Bechtolsheim Fellow), Stanford Department of Electrical Engineering Fellowship, the John W. Tukey Award from the American Statistical Association, G. David Forney Award, and the George B. Wood Legacy Prize. His publications have received over 1000 citations in the Web of Science Citation Index.

RIFAT ORHAN ÇIKMAZEL is a senior-year student in the Department of Electrical and Electronics Engineering at Yaşar University in Izmir, Turkey, where he has received an Academic Achievement Scholarship for his undergraduate education. During his junior year, he worked as a Research Scholar in the Scientific Research Project "Development of Channel Models and Techniques for Visible Light Communication" at Yaşar University. His senior design project focuses on position tracking and prediction of mobile IoT devices via machine learning methods. His current research interests are Visible Light Communication, indoor localization, and machine learning.

KEMAL HOCAOĞLU obtained his B.Sc. degree with graduation rank # 1 as a High Honor Student from the Department of Electrical and Electronics Engineering at Yaşar University in 2019. He had received a merit-based %100 Scholarship for his undergraduate education at the same university. During his senior year, he worked as a Research Scholar in the Scientific Research Project "Development of Channel Models and Techniques for Visible Light Communication" at Yaşar University. His graduation project, entitled "Video Transmission via Visible Light Communication," was supported by TÜBİTAK (Scientific and Technological Research Council of Turkey) under the 2209-B Industry Focused Undergraduate Thesis Support Program. His team's low-cost VLC system design was published at the 2019 Conference on Innovations in Intelligent Systems and Applications. His research interests are Visible Light Communication and its applications in smart cities.

ALPER SAYLAM is a senior-year student on a %100 merit-based scholarship in the Department of Electrical and Electronics Engineering at Yaşar University. His current rank in the department is # 1. During his junior year, he worked as a Research Scholar in the Scientific Research Project, entitled "Development of Channel Models and Techniques for Visible Light Communication" at Yaşar University. His senior design project is entitled "Artificial Intelligence Enabled Position Tracking and Prediction of Mobile IoT Devices in a Smart Factory Environment." His current research interests are Visible Light Communication, artificial intelligence, and indoor positioning.

• • •